


Geophysical Research Letters[®]



RESEARCH LETTER

10.1029/2023GL106995

Satellite Clear-Sky Observations Overestimate Surface Urban Heat Islands in Humid Cities

Qiquan Yang^{1,2,3} , Yi Xu¹ , Dawei Wen⁴, Ting Hu⁵, TC Chakraborty⁶, Yue Liu⁷, Rui Yao⁸, Shurui Chen², Changjiang Xiao^{2,3} , and Jie Yang⁸

¹State Key Laboratory of Lunar and Planetary Sciences, Macau University of Science and Technology, Macau, China,

²College of Surveying & Geo-Informatics, Tongji University, Shanghai, China, ³The Shanghai Key Laboratory of Space Mapping and Remote Sensing for Planetary Exploration, Tongji University, Shanghai, China, ⁴School of Computer Science and Engineering, Hubei Key Laboratory of Intelligent Robot, Wuhan Institute of Technology, Wuhan, China, ⁵School of Remote Sensing and Geomatics Engineering, Nanjing University of Information Science and Technology, Nanjing, China, ⁶Pacific Northwest National Laboratory, Richland, WA, USA, ⁷Guangzhou Institute of Geography, Guangdong Academy of Sciences, Guangzhou, China, ⁸School of Remote Sensing and Information Engineering, Wuhan University, Wuhan, China

Key Points:

- Clear-sky surface urban heat island intensity (SUHII) shows higher values and stronger spatiotemporal variations than all-sky SUHII, notably in summer, daytime, and humid areas
- The annual daytime SUHII for tropical cities is, on average, overestimated by 30% when relying on clear-sky land surface temperature (LST) observations
- Differences in clear-sky and all-sky SUHIIs can be explained by more missing LST data caused by increased clouds in urban areas

Supporting Information:

Supporting Information may be found in the online version of this article.

Correspondence to:

Y. Xu,
yixu@must.edu.mo

Citation:

Yang, Q., Xu, Y., Wen, D., Hu, T., Chakraborty, T., Liu, Y., et al. (2024). Satellite clear-sky observations overestimate surface urban heat islands in humid cities. *Geophysical Research Letters*, 51, e2023GL106995. <https://doi.org/10.1029/2023GL106995>

Received 25 OCT 2023

Accepted 25 DEC 2023

Author Contributions:

Conceptualization: Qiquan Yang

Data curation: Yue Liu

Formal analysis: Qiquan Yang

Funding acquisition: Qiquan Yang,

Yi Xu

Investigation: Qiquan Yang, TC

Chakraborty

Methodology: Qiquan Yang, Dawei Wen

Resources: Rui Yao

Software: Ting Hu

Supervision: Yi Xu

Abstract Satellite-based thermal infrared (TIR) land surface temperature (LST) is hindered by cloud cover and is applicable solely under clear-sky conditions for estimating surface urban heat island intensity (SUHII). Clear-sky SUHII may not accurately represent all-sky conditions, potentially introducing quantitative biases in assessing urban heat islands. However, the differences between clear-sky and all-sky SUHIIs and their spatiotemporal variations are still poorly understood. Our analysis of over 600 global cities demonstrates that clear-sky SUHII is mostly higher than all-sky SUHII, particularly in summer, daytime, and precipitation-rich regions. Besides, clear-sky SUHII typically exhibits stronger seasonal and diurnal contrasts than all-sky SUHII, especially for cities located in humid regions. These discrepancies can be attributed mainly to the increased missing LST data caused by cloud enhancement in urban areas. Our findings highlight the tendency for clear-sky observations to overestimate SUHII, providing valuable insights for standardizing the quantification of surface urban heat islands.

Plain Language Summary Surface urban heat island intensity (SUHII) and its spatial and temporal variations are important for describing the urban thermal environment. SUHII is usually estimated from remotely sensed land surface temperature (LST), which is only available under clear-sky conditions. The SUHII derived from clear-sky observations may differ from the SUHII under all-sky conditions. However, there is currently a lack of large-scale quantitative assessments addressing the differences between clear-sky and all-sky SUHIIs. This study fills this research gap and indicates a substantial overestimation of SUHII in humid regions when using clear-sky LST. This overestimation can be explained by the increased occurrence of missing LST data caused by the enhanced presence of clouds in urban areas. Our findings show the importance of utilizing all-sky LST data in the examination of urban surface thermal environments, especially for cities situated in humid regions.

1. Introduction

Land cover alterations and increased anthropogenic activities in the urbanization process typically lead to elevated temperatures within urban regions, thereby giving rise to the urban heat island (UHI) phenomenon (L. Li et al., 2023; Luysaert et al., 2014; Sun et al., 2016; D. Zhou et al., 2019). The UHI effect has attracted substantial attention owing to its far-reaching consequences on the local microclimate, energy consumption, vegetation growth, and the health status of urban dwellers (Chakraborty et al., 2022; Cuerdo-Vilches et al., 2023; Ho et al., 2023; X. Li et al., 2019; W. Liu et al., 2016; X. Peng et al., 2023; X. Yang et al., 2020). Thermal infrared (TIR) remote sensing techniques implemented on satellite observations can retrieve spatially continuous urban surface temperatures (Z. L. Li et al., 2013; Wan, 2014; X. Xu et al., 2023; Zheng et al., 2019). Hence, TIR land surface temperature (LST) observations have been widespread utilized in the exploration of surface UHI (SUHI) effect (Chakraborty & Lee, 2019; Clinton & Gong, 2013; Cui et al., 2021; Gui et al., 2019; S. Peng et al., 2012; Q. Yang et al., 2021; S. Zhao et al., 2016; D. Zhou et al., 2014, 2016, 2019; B. Zhou et al., 2017).

However, TIR sensors have the limitation of only capturing land surface data under clear-sky (i.e., cloudless) conditions, thereby leading to missing values in the retrieved LST data (Z. L. Li et al., 2013; Mo et al., 2021).

© 2024. The Authors.

This is an open access article under the terms of the [Creative Commons Attribution-NonCommercial-NoDerivs License](https://creativecommons.org/licenses/by/4.0/), which permits use and distribution in any medium, provided the original work is properly cited, the use is non-commercial and no modifications or adaptations are made.

Visualization: Qiquan Yang
Writing – original draft: Qiquan Yang
Writing – review & editing: Qiquan Yang, Yi Xu, Dawei Wen, Ting Hu, TC Chakraborty, Yue Liu, Rui Yao, Shurui Chen, Changjiang Xiao, Jie Yang

Global cloud cover statistics reveal that over half of the Earth's terrestrial surface is obscured by clouds (King et al., 2013), consequently leading to the presence of extensive and unevenly distributed gaps of clear-sky LST images (Mo et al., 2021). Additionally, urban areas often manifest increased cloud coverage (Qian et al., 2022; Vo et al., 2023), which exacerbates the scarcity of available clear-sky observations for SUHI analysis. Consequently, using clear-sky LST observations may pose challenges in accurately characterizing SUHI effects, potentially leading to analysis results that are skewed toward clear-sky conditions and not representative of all-sky conditions. In light of the limitations associated with clear-sky LST observations, many research efforts have been dedicated to developing algorithms for reconstructing all-sky (or, in other words, all-weather) LST data sets (Mo et al., 2021). Existing studies have facilitated the production of all-sky LST products across a variety of spatial scales—from local to national to global (Yao et al., 2023; Yu et al., 2022; X. Zhang et al., 2021).

The availability of these all-sky LST data sets offers the opportunity for quantitative comparisons between surface thermal properties under clear-sky and all-sky conditions. For example, S. Xu et al. (2023) conducted a comparison between clear-sky LST products from the Moderate Resolution Imaging Spectroradiometer (MODIS) and corresponding all-sky LST data sets in the Heihe River Basin. Their results emphasized noticeable day-night fluctuations in both the sign and magnitude of the difference between clear-sky and all-sky LSTs. Gallo and Krishnan (2022) identified noteworthy seasonal variations in the differences between clear-sky and all-sky LSTs based on a comparative analysis involving the MODIS LST products and in-situ LST observations. The global-scale analysis by Ermida et al. (2019) highlighted the spatial heterogeneity in the difference between clear-sky and all-sky LSTs, with relatively lower differences in arid zones and more pronounced differences in mid-latitudes. However, the above studies lack comparative analyses between urban and rural areas, which are crucial for discerning differences in the SUHI effect under clear-sky and all-sky conditions. Liao et al. (2022) derived clear-sky and all-sky SUHI intensities (SUHIs) for five Chinese megacities by calculating corresponding average LST difference between urban and rural areas. Their analysis revealed that clear-sky SUHI tended to be greater than all-sky SUHI, but the extent of this difference varied among cities and seasons. The localized-scale examinations underscore the potential for bias in the estimated SUHI when derived from clear-sky LST data. However, it remains questionable whether such localized conclusions, drawn from a few cities, can be extrapolated to global cities distributed in different climate zones, given the large spatiotemporal heterogeneity of the SUHI effect. Although some studies have analyzed the effect of missing LST data on SUHI estimations at continental or global scales (K. Li et al., 2022; Q. Yang et al., 2023b), there is a lack of large-scale quantitative assessments comparing SUHI derived from clear-sky and all-sky conditions.

Hence, this study collected the MODIS clear-sky LST products and corresponding all-sky LST data sets and compared SUHIs under clear-sky and all-sky conditions across 639 global cities. The objectives of this study are:

1. to quantify the differences between clear-sky and all-sky SUHIs, and
2. to analyze their spatiotemporal variations and possible drivers.

Our results yield valuable insights into the uncertainty associated with commonly performed clear-sky SUHI estimations and may help with future standardizations for detecting the SUHI effect.

2. Data and Methods

2.1. Data

The determination of urban areas relies on the Global Urban Boundary (GUB) data set developed by X. Li et al. (2020). The original GUB patches (2015) situated within a proximity of less than 2 km were merged into the same urban clusters (Lai et al., 2021b; Q. Yang et al., 2023b; C. Yang & Zhao, 2023). A total of 639 urban clusters (>100 km²) were randomly selected for representing urban areas within cities. They are distributed across four climate zones: tropical (52), arid (120), temperate (309), and cold (158) (Figure S1 in Supporting Information S1). The spatial extent of each climate zone was determined based on the major climate classes identified by the Köppen-Geiger climate scheme (Beck et al., 2018).

All-sky LST was derived from the Global Seamless and High-resolution Temperature Data set (GSHTD) produced by Yao et al. (2023). The GSHTD can provide global seamless LST data under all-sky conditions with a spatial resolution of 1 km. Consistent with the all-sky LST, the clear-sky LST was derived from the MODIS LST products (MOD11A2). The all-sky and clear-sky LST data sets maintain uniformity in their spatial extent,

covering the entire globe, as well as in their temporal range, spanning from 2014 to 2016. These data sets were subjected to separate annual and seasonal averaging as part of our analysis.

The surface elevation was obtained from the Global 30 Arc-Second Elevation (GTOPO30) data and used to minimize the influence of topographic relief on the estimation of SUHII. The nighttime light intensity was acquired from the Visible Infrared Imaging Radiometer Suite Day/Night Band (VIIRS DNB) product and applied for minimizing the uncertainty in SUHII estimations caused by human activity. The surface water was derived from Global Surface Water data set developed by Pekel et al. (2016) and utilized to eliminate the influence of water bodies on the estimation of SUHII. The annual precipitation, calculated from the TerraClimate data set (Abatzoglou et al., 2018), was employed to assess the general level of wetness or dryness of cities. The details for the aforementioned data are presented in Text S1 and Table S1 in Supporting Information S1.

2.2. Analysis

2.2.1. Estimation of SUHII

SUHII is defined as the average LST difference between the urban area and its surrounding rural area. Currently, various methods exist for estimating SUHII, with differences primarily arising from the definition of rural area (K. Li et al., 2022; Q. Yang et al., 2023b). The preferred rural area should be chosen to minimize the effects of natural factors like topographic relief and water bodies, while also eliminating the influence of human activities (K. Li et al., 2022). Hence, this study utilized the Modified Equal Area-Rural (MEA-R) method, as introduced by K. Li et al. (2022), to extract the rural area. This method has been proved to be effective in removing the influence of confounding factors on the estimation of SUHII (K. Li et al., 2022). Specific details of the MEA-R method are provided in Text S1 in Supporting Information S1. After obtaining the rural area, we calculated both the average LST of the urban area (LST_U) and the average LST of the rural area (LST_R). SUHII can then be determined using the following formula:

$$SUHII = LST_U - LST_R \quad (1)$$

2.2.2. Comparison Analysis Between Clear-Sky and All-Sky SUHII

For each city, we calculated the clear-sky average LST within the urban area ($LST_{U_Clearsky}$) and the rural area ($LST_{R_Clearsky}$), as well as the all-sky average LST within the urban area (LST_{U_Allsky}) and the rural area (LST_{R_Allsky}). Then, we can get the clear-sky SUHII ($SUHII_{Clearsky}$) and the all-sky SUHII ($SUHII_{Allsky}$) according to Equation 1. After that, we can also obtain the following formulas:

$$\Delta SUHII = SUHII_{Clearsky} - SUHII_{Allsky} \quad (2)$$

$$\Delta LST_U = LST_{U_Clearsky} - LST_{U_Allsky} \quad (3)$$

$$\Delta LST_R = LST_{R_Clearsky} - LST_{R_Allsky} \quad (4)$$

where $\Delta SUHII$ represents the difference between clear-sky and all-sky SUHII. Similarly, ΔLST_U and ΔLST_R represent the difference between clear-sky and all-sky average LSTs within the urban area and the rural area, respectively. We calculated all above metrics across 639 global cities and conducted an analysis of their spatial, seasonal, and diurnal variations.

2.2.3. Calculation of the Missing Rate of Clear-Sky LST

It is widely acknowledged that clear-sky LST is susceptible to disturbances such as clouds, and as a result, it may experience data gaps or missing data issues. To assess the extent of missing data in the clear-sky LST data set, we computed a metric known as the missing rate (MR) similar to Chakraborty et al. (2020). For a specific pixel within the urban area or the rural area, assuming that the number of LST images is N and the number of available clear-sky LST observations is n , the MR for that pixel can be expressed as follows:

$$MR = (N - n)/N \times 100\% \quad (5)$$

The MR ranges from 0% to 100%, with larger value indicating more severe data missing in the clear-sky LST data set. For each city, we calculated the average MR for all pixels located in the urban area (MR_U) and the rural area (MR_R), respectively, and further calculated their difference (MR_{Diff}). We examined their correlations with

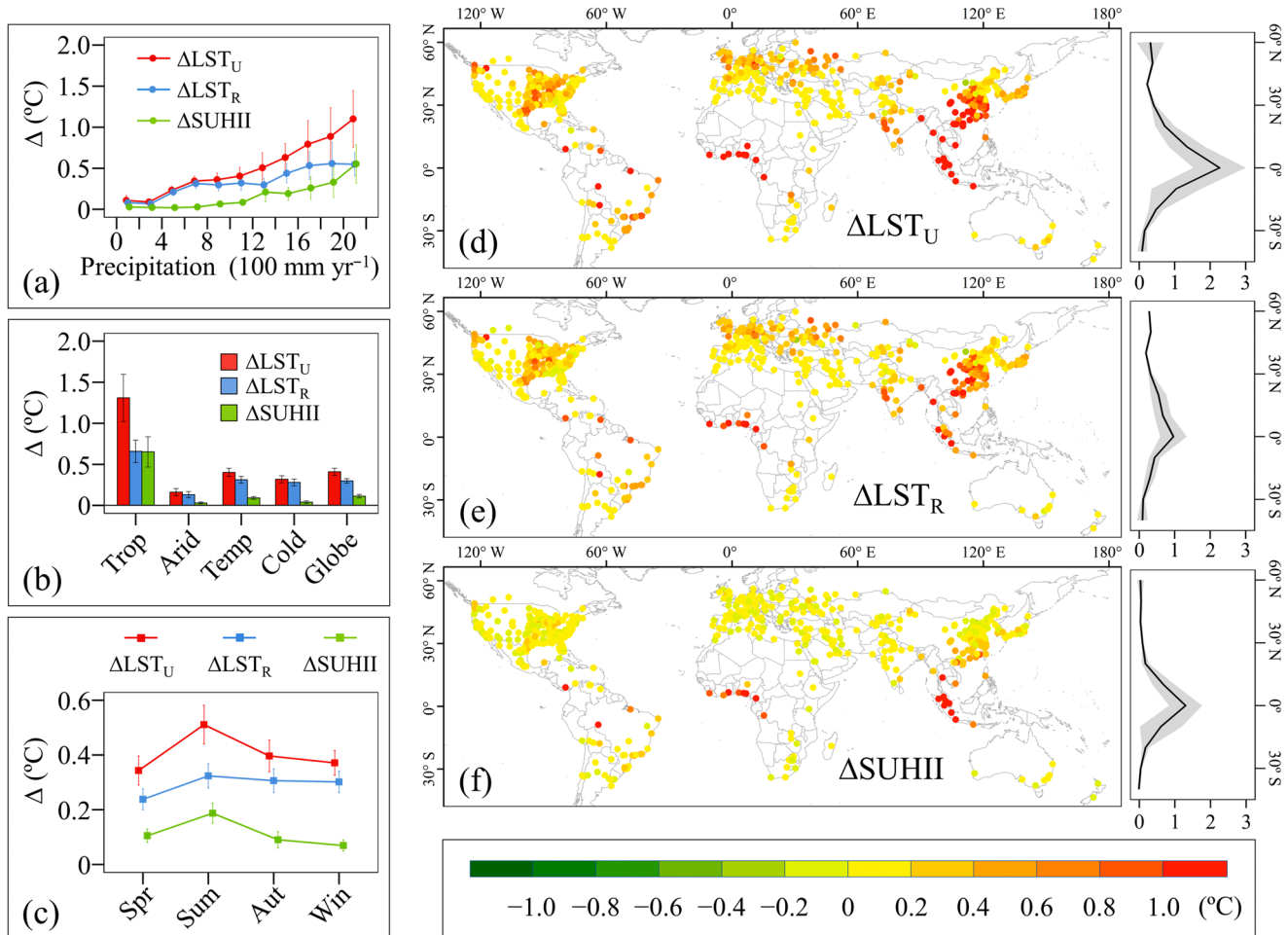


Figure 1. Clear-sky and all-sky differences in surface urban heat island intensity (SUHII) (Δ SUHII), urban average land surface temperature (LST) (Δ LST_U), and rural average LST (Δ LST_R). (a) Annual daytime averages of different precipitation intervals. (b) Annual daytime averages for different climate zones (tropical zone [Trop], arid zone [Arid], temperate zone [Temp], and cold zone [Cold]). (c) Daytime averages for global cities across seasons (spring [Spr], summer [Sum], autumn [Aut], and winter [Win]). (d–f) Spatial distributions of annual daytime Δ LST_U, Δ LST_R, and Δ SUHII. Error bars in (a)–(c) and shaded areas in (d)–(f) represent 95% confidence intervals. The nighttime results display similar spatiotemporal patterns to the daytime results, please refer to Figure S2 in Supporting Information S1.

Δ LST_U, Δ LST_R, and Δ SUHII, aiming to offer plausible explanations for the difference between clear-sky and all-sky SUHIs.

3. Results

3.1. Spatiotemporal Variations of the Difference Between Clear-Sky and All-Sky SUHIs

In general, clear-sky SUHII tends to be higher than all-sky SUHII. On a global average, the annual daytime and nighttime clear-sky SUHIs reach $1.23 \pm 0.12^\circ\text{C}$ (95% confidence interval, hereinafter) and $1.31 \pm 0.05^\circ\text{C}$, respectively, which are significantly ($p < 0.05$, t -test) higher compared to the corresponding all-sky SUHIs of $1.12 \pm 0.12^\circ\text{C}$ and $1.27 \pm 0.05^\circ\text{C}$ (Table S2 in Supporting Information S1). The difference between clear-sky SUHII and all-sky SUHII, denoted as Δ SUHII, displays clear spatial and temporal variations.

It is evident that both daytime and nighttime Δ SUHIs show a notable rise as latitude decreases (Figure 1, Figure S2 in Supporting Information S1). As a result, cities with higher Δ SUHII are concentrated in regions like Southeast Asia, Central Africa, and the Caribbean, which are situated near the equator. The precipitation grouping statistics reveal a noteworthy trend: Δ SUHII substantially increases with higher annual precipitation levels (Figure 1a). This suggests that relying on clear-sky LST observations would result in a noticeable overestimation of SUHII for cities located in regions with more precipitation. Consequently, Δ SUHII tends to be much larger

for cities located in the precipitation-rich tropical zone compared to cities in other climate zones (Figure 1b). On average, daytime and nighttime Δ SUHII in the tropical zone reach $0.65 \pm 0.18^\circ\text{C}$ and $0.21 \pm 0.06^\circ\text{C}$, respectively. These values are approximately 5–6 times higher than the global averages and significantly greater than in other climate zones (Table S2 in Supporting Information S1). Overall, the usage of clear-sky LST data results in an overestimation of approximately 30% for annual daytime SUHII and 20% for annual nighttime SUHII in the tropical zone when compared to using all-sky LST data (Table S2 in Supporting Information S1).

It is found that Δ SUHII demonstrates a notable diurnal and seasonal variation, characterized by higher values during daytime compared to nighttime and a stronger presence during the summer season relative to the winter season (Figure 1, Figure S2 and Table S3 in Supporting Information S1). Globally, on average, the annual daytime Δ SUHII reaches $0.11 \pm 0.02^\circ\text{C}$, much higher than the annual nighttime Δ SUHII of $0.04 \pm 0.00^\circ\text{C}$, and the summer daytime Δ SUHII is $0.19 \pm 0.04^\circ\text{C}$, surpassing the winter daytime Δ SUHII of $0.07 \pm 0.02^\circ\text{C}$. In addition, the use of clear-sky LST data not only leads to an overestimation of SUHII itself, but also amplifies the day-night differences and seasonal contrasts of SUHII (Table S3 in Supporting Information S1). For instance, on a global average, clear-sky SUHII during the summer demonstrates a day-night difference of $0.56 \pm 0.18^\circ\text{C}$, surpassing the day-night difference observed in summertime all-sky SUHII ($0.47 \pm 0.17^\circ\text{C}$). Similarly, the global average of summer-winter difference in daytime clear-sky SUHII reaches $1.49 \pm 0.14^\circ\text{C}$, which is higher than that of all-sky SUHII ($1.37 \pm 0.14^\circ\text{C}$). More importantly, the amplifying effect of clear-sky LST observations on the seasonal and diurnal contrasts of SUHII appears to be more pronounced in regions characterized by higher precipitation, such as the tropical zone (Table S3 in Supporting Information S1).

3.2. Drivers for the Difference Between Clear-Sky and All-Sky SUHIIs

It can be observed that, on average, clear-sky LST tends to be higher than all-sky LST both within the urban area and the rural area (Figure 1, Figure S2 in Supporting Information S1). This suggests that employing clear-sky LST data potentially leads to an overestimation of average LST, and this overestimation is more pronounced in the urban area. Consequently, it leads to an overall higher value of Δ LST_U compared to Δ LST_R, accompanied by a corresponding positive value of Δ SUHII. This provides a reasonable explanation for the clear-sky overestimation of the SUHII estimations. Additionally, although Δ LST_U and Δ LST_R exhibit similar spatiotemporal patterns, Δ LST_U displays a greater degree of variability, particularly in humid regions and during the summer daytime (Figure 1). This coincides with the spatiotemporal variation observed in Δ SUHII.

Further analysis reveals that MR of clear-sky LST data in the urban area (i.e., MR_U) is generally higher than that in the rural area (i.e., MR_R) (Figure S3 in Supporting Information S1), which aligns with the higher value of Δ LST_U compared to Δ LST_R. Besides, the difference between MR_U and MR_R (i.e., MR_{Diff}) exhibits a consistent spatiotemporal pattern with Δ SUHII, which is also shown to be stronger during summer daytime in the humid cities (Figure S3 in Supporting Information S1). More importantly, Δ SUHII displays a significant positive correlation with MR_{Diff}, which further highlights the significance of missing data as a factor driving the clear-sky and all-sky discrepancies (Figure 2).

4. Discussion

Remotely sensed LST data from observations in the thermal infrared plays a crucial role in studying the urban surface thermal environment. However, it is limited to capturing observations during clear-sky conditions, which presents a challenge in accurately representing the SUHI effect. This study offers an extensive comparative analysis of clear-sky and all-sky SUHIIs, as well as an examination of their underlying drivers in global cities. Our findings offer valuable insights for current research, which can be summarized in the following two aspects.

4.1. Our Results Provide Direct Evidence for the Clear-Sky Overestimation of SUHI Effect in Humid Regions

It is found that utilizing clear-sky LST data not only leads to an overestimation of the SUHII but also amplifies its diurnal and seasonal contrasts when compared to the use of all-sky LST data. Moreover, these clear-sky overestimations exhibit spatial variability, with more pronounced effects observed in regions characterized by higher levels of precipitation. Specifically, for cities located in the tropical zone, the annual daytime and

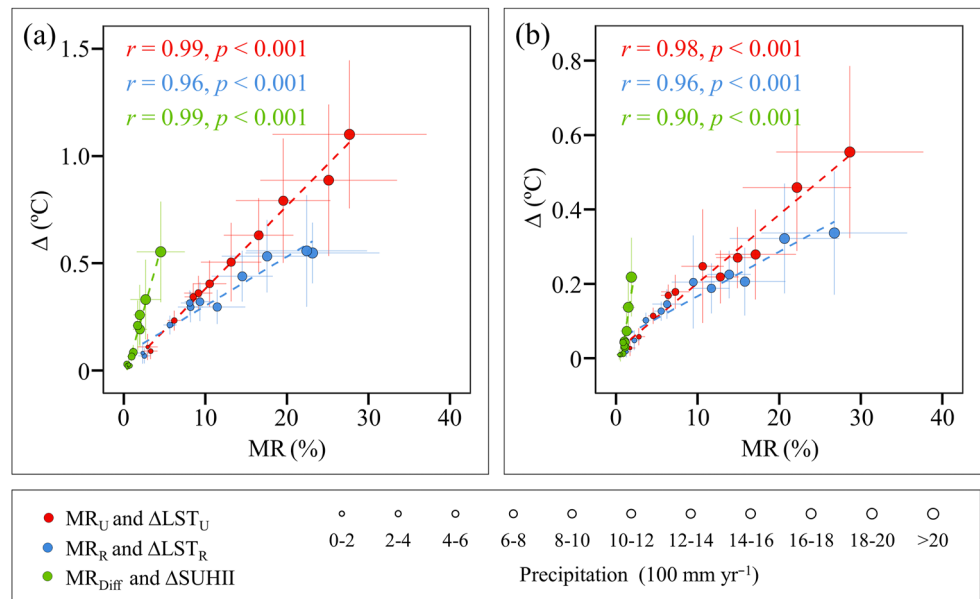


Figure 2. Relations between Δ SUHII and MR_{Diff} , ΔLST_U and MR_U , and ΔLST_R and MR_R . (a) Annual daytime results. (b) Annual nighttime results. Δ SUHII, ΔLST_U , and ΔLST_R represent clear-sky and all-sky differences in surface urban heat island intensity (SUHII), urban average land surface temperature (LST), and rural average LST, respectively. MR_U and MR_R refer to missing rate of clear-sky LST observations for the urban area and the rural area, respectively. The difference between MR_U and MR_R is represented as MR_{Diff} . r and p represent Pearson's correlation coefficient and significance level, respectively. The colored points and error bars represent the mean values and 95% confidence intervals, respectively.

nighttime SUHII can be, on average, overestimated by about 30% and 20%, respectively, when using the clear-sky LST observations. Though previous studies have identified the bias resulting from using clear-sky LST data (Ermida et al., 2019; Gallo & Krishnan, 2022; S. Xu et al., 2023), there remains a lack of large-scale analyses specifically focusing on the urban-rural difference (i.e., SUHII). This study addresses this research gap by conducting quantitative analysis on a global scale, offering direct evidence for the overestimation of the SUHI effect when relying on the LST observations under clear-sky conditions. More crucially, existing studies investigating the spatiotemporal patterns and driving factors of the SUHI effect primarily rely on clear-sky LST data (Cao et al., 2016; Chakraborty & Lee, 2019; Clinton & Gong, 2013; Du et al., 2023; Gui et al., 2019; Imhoff et al., 2010; Lai et al., 2018b, 2021a; X. Li et al., 2023; Y. Liu et al., 2021, 2023; Z. Liu et al., 2022a, 2022b; S. Peng et al., 2012; Quan et al., 2016; Q. Yang et al., 2017, 2019, 2023a; C. Yang & Zhao, 2023; Yao, Wang, Huang, Chen, et al., 2018; Yao et al., 2019; B. Zhou et al., 2013, 2017; D. Zhou et al., 2014, 2016). The findings from these studies could benefit from the updates to integrate the differences in their spatial patterns between clear-sky and all-sky SUHII. In particular, several studies have tried to explain the SUHI patterns from climatic perspectives (L. Li et al., 2020; Manoli et al., 2019; L. Zhao et al., 2014). It is especially crucial for such studies to account for the distinctions between clear-sky and all-sky SUHII, given the high dependence of the clear-sky bias on precipitation levels. Fortunately, a succession of all-sky LST data sets is now becoming available (Mo et al., 2021; Shiff et al., 2021; Yao et al., 2023; Yu et al., 2022; X. Zhang et al., 2021), offering a new opportunity to gain a more accurate comprehension of the SUHI patterns and their driving factors.

4.2. Our Results Unveil a Potential Mechanism That Explains the Discrepancies Between Clear-Sky and All-Sky SUHII

The amount of clouds can be influenced by atmospheric moisture, temperature, wind patterns, solar radiation, and the presence of weather systems, with their interplay determining cloud formation and dissipation (Bony et al., 2015; Schiro et al., 2022; Su et al., 2017). Urban areas typically exhibit higher cloud cover due to a confluence of influential factors (Qian et al., 2022; Vo et al., 2023). The increased aerodynamic roughness within urban landscapes, resulting from the presence of buildings and other structures, induces local atmospheric disturbances that facilitate heightened cloud formation (Rajeswari et al., 2021). Moreover, the heightened temperatures

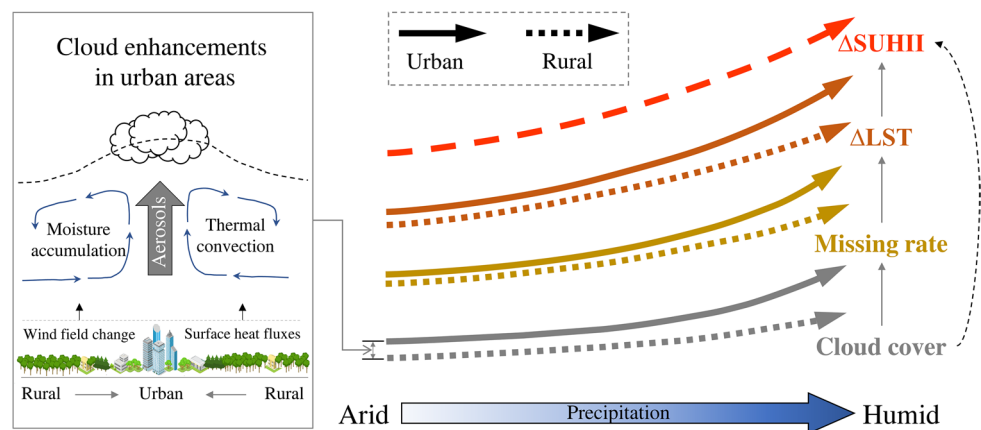


Figure 3. Schematic illustration of the mechanisms behind the clear-sky and all-sky surface urban heat island intensity (SUHII) differences and their spatial variations. The heightened cloud cover in urban areas poses more challenges for satellite observations, resulting in a higher differences between clear-sky and all-sky land surface temperatures (LSTs) compared to rural areas. This urban-rural contrast further contributes to the difference between clear-sky and all-sky SUHIIs. The enhancement of urban clouds is more pronounced in cities with a higher level of precipitation, accentuating the contrast between clear-sky and all-sky SUHIIs in humid areas compared to arid regions.

associated with surface heating in urban areas can impact atmospheric dynamics, fostering the condensation of water vapor into clouds (Chen et al., 2011; Vo et al., 2023). Additionally, the augmented concentration of anthropogenic emissions in urban settings, stemming from industrial activities and vehicular traffic, introduces additional particulate matter and aerosols into the atmosphere (Z. H. Zhang et al., 2017). These pollutants serve as cloud condensation nuclei, providing surfaces for water droplets to coalesce and thereby amplifying cloud cover (Leng et al., 2013; Ma et al., 2010). This intricate interplay among urban characteristics, atmospheric conditions, and human activities underscores the nuanced relationship between urbanization and the prevalence of clouds, distinguishing urban areas from their rural counterparts. The heightened cloud cover causes a more severe missing of satellite TIR temperature data in urban areas, which is consistent with our observations and previous estimates (Chakraborty et al., 2020). Recent evidence suggests that an increased presence of clouds can reduce surface heating by solar radiation, leading to a generally lower all-sky LST than clear-sky LST (Ghausi et al., 2023). As a result, more cloudiness in urban areas would cause a greater difference between clear-sky and all-sky LSTs. This offers a plausible explanation for the higher clear-sky SUHII compared to the all-sky SUHII. More importantly, the enhancement of urban cloud appears to be more pronounced in wetter areas (Vo et al., 2023), as substantiated by the observed increase in MR_{Diff} with higher levels of precipitation (Figure S3 in Supporting Information S1). Consequently, the differences between clear-sky and all-sky SUHIIs are more pronounced in humid regions compared to dry regions. This elucidates why the overestimation of SUHII is more conspicuous when utilizing clear-sky LST in humid areas. Moreover, the spatiotemporal patterns of $\Delta SUHII$ consistently align with those of MR_{Diff} (Figure 2). This further supports our hypothesis that the increased cloud cover in urban areas, indicated by a higher occurrence of missing data, results in a more substantial contrast between clear-sky and all-sky LSTs in the urban area compared to the rural area, ultimately manifesting as a clear-sky overestimation in SUHII. Building on the aforementioned hypothesis, we have created a schematic diagram illustrating the factors behind the discrepancies in clear-sky and all-sky SUHIIs and showing potential reasons for their variations with precipitation levels (Figure 3).

This study is subject to certain inherent constraints and limitations. First, this study relies on the newly released all-sky LST data sets produced by Yao et al. (2023). Due to the absence of accuracy assessments for individual LST pixels, our analysis does not address the impact of uncertainty in the LST data on our results. Second, to fully utilize the available MODIS LST data, Yao et al. (2023) did not employ any filtering process when generating the all-sky LST data sets. Consistent with their practices, we also used all the available clear-sky MODIS LST pixels to ensure fairness in our comparison. The unfiltered low-precision LST data may introduce uncertainties when estimating SUHII (Lai et al., 2018a). However, these uncertainties are implausible to impact the difference between clear-sky and all-sky SUHIIs as they offset each other during the differencing process. Third, our analysis relied on LST observations from the Terra sensor, as Yao et al. (2023) developed their all-sky

LST based on Terra LST products. Currently, Aqua LST products are commonly utilized in UHI-related studies because of their proximity to daily maximum and minimum temperatures. Differences between Terra and Aqua LSTs can influence SUHII estimations (Yao, Wang, Huang, Niu, et al., 2018). However, variations in SUHII due to sensor differences are unlikely to significantly affect our results, as our focus lies in discerning differences between clear-sky and all-sky SUHIIs. Finally, this study scrutinizes the mechanisms underlying the discrepancies between clear-sky and all-sky SUHIIs, primarily focusing on the aspect of missing data attributed to cloud cover. Nevertheless, it is imperative to acknowledge that cloud cover not only leads to missing data but also instigates alterations in surface energy fluxes, thereby influencing surface temperature and, consequently, the intensity of heat islands. Future research efforts could combine more data (e.g., flux tower and reanalysis data) with different analytical methods (statistical and modeling approaches) to make a more in-depth analysis of the factors contributing to the difference between clear-sky and all-sky SUHIIs.

Data Availability Statement

The data used in this study is available at Q. Yang (2023).

Acknowledgments

This research was supported by the Macau Young Scholars Program (AM2022001), the National Natural Science Foundation of China (42201389), the Science and Technology Development Fund of Macau (0014/2022/A1 and 0005/2020/A1), and the Postdoctoral Science Foundation of China (2021TQ0245 and 2021M702470). TC's contribution was supported by a U.S. Department of Energy Office of Science Early Career grant and a NASA Interdisciplinary Research in Earth Science grant. PNNL is operated for the Department of Energy by Battelle Memorial Institute under contract DE-AC05-76RL01830.

References

- Abatzoglou, J. T., Dobrowski, S. Z., Parks, S. A., & Hegewisch, K. C. (2018). TerraClimate, a high-resolution global dataset of monthly climate and climatic water balance from 1958–2015. *Scientific Data*, 5(1), 170191. <https://doi.org/10.1038/sdata.2017.191>
- Beck, H. E., Zimmermann, N. E., McVicar, T. R., Vergopolan, N., Berg, A., & Wood, E. F. (2018). Present and future Köppen-Geiger climate classification maps at 1-km resolution. *Scientific Data*, 5(1), 180214. <https://doi.org/10.1038/sdata.2018.214>
- Bony, S., Stevens, B., Frierson, D. M., Jakob, C., Kageyama, M., Pincus, R., et al. (2015). Clouds, circulation and climate sensitivity. *Nature Geoscience*, 8(4), 261–268. <https://doi.org/10.1038/ngeo2398>
- Cao, C., Lee, X., Liu, S., Schultz, N., Xiao, W., Zhang, M., & Zhao, L. (2016). Urban heat islands in China enhanced by haze pollution. *Nature Communications*, 7(1), 12509. <https://doi.org/10.1038/ncomms12509>
- Chakraborty, T., Hsu, A., Many, D., & Sheriff, G. (2020). A spatially explicit surface urban heat island database for the United States: Characterization, uncertainties, and possible applications. *ISPRS Journal of Photogrammetry and Remote Sensing*, 168, 74–88. <https://doi.org/10.1016/j.isprsjprs.2020.07.021>
- Chakraborty, T., & Lee, X. (2019). A simplified urban-extent algorithm to characterize surface urban heat islands on a global scale and examine vegetation control on their spatiotemporal variability. *International Journal of Applied Earth Observation and Geoinformation*, 74, 269–280. <https://doi.org/10.1016/j.jag.2018.09.015>
- Chakraborty, T., Venter, Z. S., Qian, Y., & Lee, X. (2022). Lower urban humidity moderates outdoor heat stress. *AGU Advances*, 3(5), e2022AV000729. <https://doi.org/10.1029/2022AV000729>
- Chen, F., Miao, S., Tewari, M., Bao, J. W., & Kusaka, H. (2011). A numerical study of interactions between surface forcing and sea breeze circulations and their effects on stagnation in the greater Houston area. *Journal of Geophysical Research*, 116(D12), D12105. <https://doi.org/10.1029/2010JD015533>
- Clinton, N., & Gong, P. (2013). MODIS detected surface urban heat islands and sinks: Global locations and controls. *Remote Sensing of Environment*, 134, 294–304. <https://doi.org/10.1016/j.rse.2013.03.008>
- Cuerdo-Vilches, T., Díaz, J., López-Bueno, J. A., Luna, M. Y., Navas, M. A., Mirón, I. J., & Linares, C. (2023). Impact of urban heat islands on morbidity and mortality in heat waves: Observational time series analysis of Spain's five cities. *Science of the Total Environment*, 890, 164412. <https://doi.org/10.1016/j.scitotenv.2023.164412>
- Cui, F., Hamdi, R., Yuan, X., He, H., Yang, T., Kuang, W., et al. (2021). Quantifying the response of surface urban heat island to urban greening in global north megacities. *Science of the Total Environment*, 801, 149553. <https://doi.org/10.1016/j.scitotenv.2021.149553>
- Du, H., Zhan, W., Voogt, J., Bechtel, B., Chakraborty, T. C., Liu, Z., et al. (2023). Contrasting trends and drivers of global surface and canopy urban heat islands. *Geophysical Research Letters*, 50(15), e2023GL104661. <https://doi.org/10.1029/2023GL104661>
- Ermida, S. L., Trigo, I. F., DaCamara, C. C., Jiménez, C., & Prigent, C. (2019). Quantifying the clear-sky bias of satellite land surface temperature using microwave-based estimates. *Journal of Geophysical Research: Atmospheres*, 124(2), 844–857. <https://doi.org/10.1029/2018JD029354>
- Gallo, K., & Krishnan, P. (2022). Evaluation of the bias in the use of clear-sky compared with all-sky observations of monthly and annual daytime land surface temperature. *Journal of Applied Meteorology and Climatology*, 61(10), 1485–1495. <https://doi.org/10.1175/JAMC-D-21-0240.1>
- Ghausi, S. A., Tian, Y., Zehe, E., & Kleidon, A. (2023). Radiative controls by clouds and thermodynamics shape surface temperatures and turbulent fluxes over land. *Proceedings of the National Academy of Sciences of the United States of America*, 120(29), e2220400120. <https://doi.org/10.1073/pnas.2220400120>
- Gui, X., Wang, L., Yao, R., Yu, D., & Li, C. A. (2019). Investigating the urbanization process and its impact on vegetation change and urban heat island in Wuhan, China. *Environmental Science and Pollution Research*, 26(30), 30808–30825. <https://doi.org/10.1007/s11356-019-06273-w>
- Ho, J. Y., Shi, Y., Lau, K. K. L., Ng, E. Y. Y., Ren, C., & Goggins, W. B. (2023). Urban heat island effect-related mortality under extreme heat and non-extreme heat scenarios: A 2010–2019 case study in Hong Kong. *Science of the Total Environment*, 858, 159791. <https://doi.org/10.1016/j.scitotenv.2022.159791>
- Imhoff, M. L., Zhang, P., Wolfe, R. E., & Bounoua, L. (2010). Remote sensing of the urban heat island effect across biomes in the continental USA. *Remote Sensing of Environment*, 114(3), 504–513. <https://doi.org/10.1016/j.rse.2009.10.008>
- King, M. D., Platnick, S., Menzel, W. P., Ackerman, S. A., & Hubanks, P. A. (2013). Spatial and temporal distribution of clouds observed by MODIS onboard the terra and aqua satellites. *IEEE Transactions on Geoscience and Remote Sensing*, 51(7), 3826–3852. <https://doi.org/10.1109/TGRS.2012.2227333>
- Lai, J., Zhan, W., Huang, F., Quan, J., Hu, L., Gao, L., & Ju, W. (2018a). Does quality control matter? Surface urban heat island intensity variations estimated by satellite-derived land surface temperature products. *ISPRS Journal of Photogrammetry and Remote Sensing*, 139, 212–227. <https://doi.org/10.1016/j.isprsjprs.2018.03.012>

- Lai, J., Zhan, W., Huang, F., Voogt, J., Bechtel, B., Allen, M., et al. (2018b). Identification of typical diurnal patterns for clear-sky climatology of surface urban heat islands. *Remote Sensing of Environment*, 217, 203–220. <https://doi.org/10.1016/j.rse.2018.08.021>
- Lai, J., Zhan, W., Quan, J., Liu, Z., Li, L., Huang, F., et al. (2021a). Reconciling debates on the controls on surface urban heat island intensity: Effects of scale and sampling. *Geophysical Research Letters*, 48(19), e2021GL094485. <https://doi.org/10.1029/2021GL094485>
- Lai, J., Zhan, W., Voogt, J., Quan, J., Huang, F., Zhou, J., et al. (2021b). Meteorological controls on daily variations of nighttime surface urban heat islands. *Remote Sensing of Environment*, 253, 112198. <https://doi.org/10.1016/j.rse.2020.112198>
- Leng, C., Cheng, T., Chen, J., Zhang, R., Tao, J., Huang, G., et al. (2013). Measurements of surface cloud condensation nuclei and aerosol activity in downtown Shanghai. *Atmospheric Environment*, 69, 354–361. <https://doi.org/10.1016/j.atmosenv.2012.12.021>
- Li, K., Chen, Y., & Gao, S. (2022). Uncertainty of city-based urban heat island intensity across 1112 global cities: Background reference and cloud coverage. *Remote Sensing of Environment*, 271, 112898. <https://doi.org/10.1016/j.rse.2022.112898>
- Li, L., Zha, Y., & Zhang, J. (2020). Spatially non-stationary effect of underlying driving factors on surface urban heat islands in global major cities. *International Journal of Applied Earth Observation and Geoinformation*, 90, 102131. <https://doi.org/10.1016/j.jag.2020.102131>
- Li, L., Zhan, W., Hu, L., Chakraborty, T. C., Wang, Z., Fu, P., et al. (2023). Divergent urbanization-induced impacts on global surface urban heat island trends since 1980s. *Remote Sensing of Environment*, 295, 113650. <https://doi.org/10.1016/j.rse.2023.113650>
- Li, X., Chakraborty, T. C., & Wang, G. (2023). Comparing land surface temperature and mean radiant temperature for urban heat mapping in Philadelphia. *Urban Climate*, 51, 101615. <https://doi.org/10.1016/j.uclim.2023.101615>
- Li, X., Gong, P., Zhou, Y., Wang, J., Bai, Y., Chen, B., et al. (2020). Mapping global urban boundaries from the global artificial impervious area (GAIA) data. *Environmental Research Letters*, 15(9), 094044. <https://doi.org/10.1088/1748-9326/ab9be3>
- Li, X., Zhou, Y., Yu, S., Jia, G., Li, H., & Li, W. (2019). Urban heat island impacts on building energy consumption: A review of approaches and findings. *Energy*, 174, 407–419. <https://doi.org/10.1016/j.energy.2019.02.183>
- Li, Z. L., Tang, B. H., Wu, H., Ren, H., Yan, G., Wan, Z., et al. (2013). Satellite-derived land surface temperature: Current status and perspectives. *Remote Sensing of Environment*, 131, 14–37. <https://doi.org/10.1016/j.rse.2012.12.008>
- Liao, Y., Shen, X., Zhou, J., Ma, J., Zhang, X., Tang, W., et al. (2022). Surface urban heat island detected by all-weather satellite land surface temperature. *Science of the Total Environment*, 811, 151405. <https://doi.org/10.1016/j.scitotenv.2021.151405>
- Liu, W., Zhang, Y., & Deng, Q. (2016). The effects of urban microclimate on outdoor thermal sensation and neutral temperature in hot-summer and cold-winter climate. *Energy and Buildings*, 128, 190–197. <https://doi.org/10.1016/j.enbuild.2016.06.086>
- Liu, Y., Huang, X., Yang, Q., & Cao, Y. (2021). The turning point between urban vegetation and artificial surfaces for their competitive effect on land surface temperature. *Journal of Cleaner Production*, 292, 126034. <https://doi.org/10.1016/j.jclepro.2021.126034>
- Liu, Y., Huang, X., Yang, Q., Jing, W., & Yang, J. (2023). Effects of landscape on thermal livability at the community scale based on fine-grained geographic information: A case study of Shenzhen. *Science of the Total Environment*, 905, 167091. <https://doi.org/10.1016/j.scitotenv.2023.167091>
- Liu, Z., Lai, J., Zhan, W., Bechtel, B., Voogt, J., Quan, J., et al. (2022a). Urban heat islands significantly reduced by COVID-19 lockdown. *Geophysical Research Letters*, 49(2), e2021GL096842. <https://doi.org/10.1029/2021GL096842>
- Liu, Z., Zhan, W., Bechtel, B., Voogt, J., Lai, J., Chakraborty, T., et al. (2022b). Surface warming in global cities is substantially more rapid than in rural background areas. *Communications Earth & Environment*, 3(1), 219. <https://doi.org/10.1038/s43247-022-00539-x>
- Luysaert, S., Jammot, M., Stoy, P. C., Estel, S., Pongratz, J., Ceschia, E., et al. (2014). Land management and land-cover change have impacts of similar magnitude on surface temperature. *Nature Climate Change*, 4(5), 389–393. <https://doi.org/10.1038/nclimate2196>
- Ma, J., Chen, Y., Wang, W., Yan, P., Liu, H., Yang, S., et al. (2010). Strong air pollution causes widespread haze-clouds over China. *Journal of Geophysical Research*, 115, D18204. <https://doi.org/10.1029/2009JD013065>
- Manoli, G., Faticchi, S., Schläpfer, M., Yu, K., Crowther, T. W., Meili, N., et al. (2019). Magnitude of urban heat islands largely explained by climate and population. *Nature*, 573(7772), 55–60. <https://doi.org/10.1038/s41586-019-1512-9>
- Mo, Y., Xu, Y., Chen, H., & Zhu, S. (2021). A review of reconstructing remotely sensed land surface temperature under cloudy conditions. *Remote Sensing*, 13(14), 2838. <https://doi.org/10.3390/rs13142838>
- Pekel, J. F., Cottam, A., Gorelick, N., & Belward, A. S. (2016). High-resolution mapping of global surface water and its long-term changes. *Nature*, 540(7633), 418–422. <https://doi.org/10.1038/nature20584>
- Peng, S., Piao, S., Ciais, P., Friedlingstein, P., Ottle, C., Bréon, F. M., et al. (2012). Surface urban heat island across 419 global big cities. *Environmental Science and Technology*, 46(2), 696–703. <https://doi.org/10.1021/es2030438>
- Peng, X., Jiang, S., Liu, S., Valbuena, R., Smith, A., Zhan, Y., et al. (2023). Long-term satellite observations show continuous increase of vegetation growth enhancement in urban environment. *Science of the Total Environment*, 898, 165515. <https://doi.org/10.1016/j.scitotenv.2023.165515>
- Qian, Y., Chakraborty, T. C., Li, J., Li, D., He, C., Sarangi, C., et al. (2022). Urbanization impact on regional climate and extreme weather: Current understanding, uncertainties, and future research directions. *Advances in Atmospheric Sciences*, 39(6), 819–860. <https://doi.org/10.1007/s00376-021-1371-9>
- Quan, J., Zhan, W., Chen, Y., Wang, M., & Wang, J. (2016). Time series decomposition of remotely sensed land surface temperature and investigation of trends and seasonal variations in surface urban heat islands. *Journal of Geophysical Research: Atmospheres*, 121(6), 2638–2657. <https://doi.org/10.1002/2015JD024354>
- Rajeswari, J. R., Srinivas, C. V., Yesubabu, V., Hari Prasad, D., & Venkatraman, B. (2021). Impacts of urbanization, aerodynamic roughness, and land surface processes on the extreme heavy rainfall over Chennai, India. *Journal of Geophysical Research: Atmospheres*, 126(10), e2020JD034017. <https://doi.org/10.1029/2020JD034017>
- Schiro, K. A., Su, H., Ahmed, F., Dai, N., Singer, C. E., Gentile, P., et al. (2022). Model spread in tropical low cloud feedback tied to overturning circulation response to warming. *Nature Communications*, 13(1), 7119. <https://doi.org/10.1038/s41467-022-34787-4>
- Shiff, S., Helman, D., & Lensky, I. M. (2021). Worldwide continuous gap-filled MODIS land surface temperature dataset. *Scientific Data*, 8(1), 74. <https://doi.org/10.1038/s41597-021-00861-7>
- Su, H., Jiang, J. H., Neelin, J. D., Shen, T. J., Zhai, C., Yue, Q., et al. (2017). Tightening of tropical ascent and high clouds key to precipitation change in a warmer climate. *Nature Communications*, 8(1), 15771. <https://doi.org/10.1038/ncomms15771>
- Sun, Y., Zhang, X., Ren, G., Zwiers, F. W., & Hu, T. (2016). Contribution of urbanization to warming in China. *Nature Climate Change*, 6(7), 706–709. <https://doi.org/10.1038/nclimate2956>
- Vo, T. T., Hu, L., Xue, L., Li, Q., & Chen, S. (2023). Urban effects on local cloud patterns. *Proceedings of the National Academy of Sciences of the United States of America*, 120(21), e2216765120. <https://doi.org/10.1073/pnas.2216765120>
- Wan, Z. (2014). New refinements and validation of the collection-6 MODIS land-surface temperature/emissivity product. *Remote Sensing of Environment*, 140, 36–45. <https://doi.org/10.1016/j.rse.2013.08.027>

- Xu, S., Wang, D., Liang, S., Liu, Y., & Jia, A. (2023). Assessment of gridded datasets of various near surface temperature variables over Heihe River Basin: Uncertainties, spatial heterogeneity and clear-sky bias. *International Journal of Applied Earth Observation and Geoinformation*, *120*, 103347. <https://doi.org/10.1016/j.jag.2023.103347>
- Xu, X., Pei, H., Wang, C., Xu, Q., Xie, H., Jin, Y., et al. (2023). Long-term analysis of the urban heat island effect using multisource Landsat images considering inter-class differences in land surface temperature products. *Science of the Total Environment*, *858*, 159777. <https://doi.org/10.1016/j.scitotenv.2022.159777>
- Yang, C., & Zhao, S. (2023). Diverse seasonal hysteresis of surface urban heat islands across Chinese cities: Patterns and drivers. *Remote Sensing of Environment*, *294*, 113644. <https://doi.org/10.1016/j.rse.2023.113644>
- Yang, Q. (2023). Data utilized in the paper by Qiquan Yang: Satellite clear-sky observations overestimate surface urban heat islands in humid cities [Dataset]. Figshare. <https://doi.org/10.6084/m9.figshare.24783060>
- Yang, Q., Huang, X., & Li, J. (2017). Assessing the relationship between surface urban heat islands and landscape patterns across climatic zones in China. *Scientific Reports*, *7*(1), 9337. <https://doi.org/10.1038/s41598-017-09628-w>
- Yang, Q., Huang, X., & Tang, Q. (2019). The footprint of urban heat island effect in 302 Chinese cities: Temporal trends and associated factors. *Science of the Total Environment*, *655*, 652–662. <https://doi.org/10.1016/j.scitotenv.2018.11.171>
- Yang, Q., Huang, X., Yang, J., & Liu, Y. (2021). The relationship between land surface temperature and artificial impervious surface fraction in 682 global cities: Spatiotemporal variations and drivers. *Environmental Research Letters*, *16*(2), 024032. <https://doi.org/10.1088/1748-9326/abdae>
- Yang, Q., Xu, Y., Tong, X., Hu, T., Liu, Y., Chakraborty, T. C., et al. (2023a). Influence of urban extent discrepancy on the estimation of surface urban heat island intensity: A global-scale assessment in 892 cities. *Journal of Cleaner Production*, *426*, 139032. <https://doi.org/10.1016/j.jclepro.2023.139032>
- Yang, Q., Xu, Y., Tong, X., Huang, X., Liu, Y., Chakraborty, T. C., et al. (2023b). An adaptive synchronous extraction (ASE) method for estimating intensity and footprint of surface urban heat islands: A case study of 254 North American cities. *Remote Sensing of Environment*, *297*, 113777. <https://doi.org/10.1016/j.rse.2023.113777>
- Yang, X., Peng, L. L. H., Jiang, Z., Chen, Y., Yao, L., He, Y., & Xu, T. (2020). Impact of urban heat island on energy demand in buildings: Local climate zones in Nanjing. *Applied Energy*, *260*, 114279. <https://doi.org/10.1016/j.apenergy.2019.114279>
- Yao, R., Wang, L., Huang, X., Cao, Q., Wei, J., He, P., et al. (2023). Global seamless and high-resolution temperature dataset (GSHTD), 2001–2020. *Remote Sensing of Environment*, *286*, 113422. <https://doi.org/10.1016/j.rse.2022.113422>
- Yao, R., Wang, L., Huang, X., Chen, J., Li, J., & Niu, Z. (2018). Less sensitive of urban surface to climate variability than rural in Northern China. *Science of the Total Environment*, *628*, 650–660. <https://doi.org/10.1016/j.scitotenv.2018.02.087>
- Yao, R., Wang, L., Huang, X., Gong, W., & Xia, X. (2019). Greening in rural areas increases the surface urban heat island intensity. *Geophysical Research Letters*, *46*(4), 2204–2212. <https://doi.org/10.1029/2018GL081816>
- Yao, R., Wang, L., Huang, X., Niu, Y., Chen, Y., & Niu, Z. (2018). The influence of different data and method on estimating the surface urban heat island intensity. *Ecological Indicators*, *89*, 45–55. <https://doi.org/10.1016/j.ecolind.2018.01.044>
- Yu, P., Zhao, T., Shi, J., Ran, Y., Jia, L., Ji, D., & Xue, H. (2022). Global spatiotemporally continuous MODIS land surface temperature dataset. *Scientific Data*, *9*(1), 143. <https://doi.org/10.1038/s41597-022-01214-8>
- Zhang, X., Zhou, J., Liang, S., & Wang, D. (2021). A practical reanalysis data and thermal infrared remote sensing data merging (RTM) method for reconstruction of a 1-km all-weather land surface temperature. *Remote Sensing of Environment*, *260*, 112437. <https://doi.org/10.1016/j.rse.2021.112437>
- Zhang, Z. H., Khlystov, A., Norford, L. K., Tan, Z. K., & Balasubramanian, R. (2017). Characterization of traffic-related ambient fine particulate matter (PM_{2.5}) in an Asian city: Environmental and health implications. *Atmospheric Environment*, *161*, 132–143. <https://doi.org/10.1016/j.atmosenv.2017.04.040>
- Zhao, L., Lee, X., Smith, R. B., & Oleson, K. (2014). Strong contributions of local background climate to urban heat islands. *Nature*, *511*(7508), 216–219. <https://doi.org/10.1038/nature13462>
- Zhao, S., Zhou, D., & Liu, S. (2016). Data concurrency is required for estimating urban heat island intensity. *Environmental Pollution*, *208*, 118–124. <https://doi.org/10.1016/j.envpol.2015.07.037>
- Zheng, X., Li, Z. L., Nerry, F., & Zhang, X. (2019). A new thermal infrared channel configuration for accurate land surface temperature retrieval from satellite data. *Remote Sensing of Environment*, *231*, 111216. <https://doi.org/10.1016/j.rse.2019.111216>
- Zhou, B., Rybski, D., & Kropp, J. P. (2013). On the statistics of urban heat island intensity. *Geophysical Research Letters*, *40*(20), 5486–5491. <https://doi.org/10.1002/2013GL057320>
- Zhou, B., Rybski, D., & Kropp, J. P. (2017). The role of city size and urban form in the surface urban heat island. *Scientific Reports*, *7*(1), 4791. <https://doi.org/10.1038/s41598-017-04242-2>
- Zhou, D., Xiao, J., Bonafoni, S., Berger, C., Deilami, K., Zhou, Y., et al. (2019). Satellite remote sensing of surface urban heat islands: Progress, challenges, and perspectives. *Remote Sensing*, *11*(1), 48. <https://doi.org/10.3390/rs11010048>
- Zhou, D., Zhang, L., Li, D., Huang, D., & Zhu, C. (2016). Climate-vegetation control on the diurnal and seasonal variations of surface urban heat islands in China. *Environmental Research Letters*, *11*(7), 074009. <https://doi.org/10.1088/1748-9326/11/7/074009>
- Zhou, D., Zhao, S., Liu, S., Zhang, L., & Zhu, C. (2014). Surface urban heat island in China's 32 major cities: Spatial patterns and drivers. *Remote Sensing of Environment*, *152*, 51–61. <https://doi.org/10.1016/j.rse.2014.05.017>